Interface free-energy exponent in the one-dimensional Ising spin glass with long-range interactions in both the droplet and broken replica symmetry regions

T. Aspelmeier,[1,2,3] Wenlong Wang,[4] M. A. Moore,[5] and Helmut G. Katzgraber[4,6]

[1]*Felix Bernstein Institute for Mathematical Statistics in the Biosciences, Georg August University of Göttingen, 37077 Göttingen, Germany*

[2]*Institute for Mathematical Stochastics, University of Göttingen, 37073 Göttingen, Germany*

[3]*Statistical Inverse Problems in Biophysics, Max Planck Institute for Biophysical Chemistry, 37077 Göttingen, Germany*

[4]*Department of Physics and Astronomy, Texas A&M University, College Station, Texas 77843-4242, USA*

[5]*School of Physics and Astronomy, University of Manchester, Manchester M13 9PL, United Kingdom*

[6]*Santa Fe Institute, 1399 Hyde Park Road, Santa Fe, New Mexico 87501, USA*

(Received 13 June 2016; published 11 August 2016)

The one-dimensional Ising spin-glass model with power-law long-range interactions is a useful proxy model for studying spin glasses in higher space dimensions and for finding the dimension at which the spin-glass state changes from having broken replica symmetry to that of droplet behavior. To this end we have calculated the exponent that describes the difference in free energy between periodic and antiperiodic boundary conditions. Numerical work is done to support some of the assumptions made in the calculations and to determine the behavior of the interface free-energy exponent of the power law of the interactions. Our numerical results for the interface free-energy exponent are badly affected by finite-size problems.

DOI: 10.1103/PhysRevE.94.022116

I. INTRODUCTION

The Edwards-Anderson (EA) Hamiltonian [1] is universally agreed to capture the essence of spin-glass behavior. However, what is not agreed upon is the nature of its low-temperature ordered state. There are two main theories. The first is the replica symmetry breaking (RSB) theory of Parisi [2–7], which is known to be correct for the Sherrington-Kirkpatrick (SK) model [8], which is the mean-field or infinite-dimensional limit of the EA model. It is characterized by a very large number of pure states that organize into an ultrametric topology [6]. On the other hand, in the second theory, the droplet picture, developed in Refs. [9–13], there are only two pure states. In this picture behavior is dominated by low-lying excitations or droplets whose (free) energies scale as their linear dimension ℓ as ℓ^{θ} and have a fractal dimension d_s where $d-1 < d_s < d$ for a d-dimensional system. In contrast, in the RSB picture there are low-lying excitations that cost an energy of $O(1)$ and are space filling, that is, $d_s = d$. Despite the striking differences of the two pictures, it has proven difficult to establish by either experiment or simulations which holds for, say, three-dimensional ($d = 3$) spin glasses.

Much of the effort in this regard has focused on the existence or absence of the de Almeida–Thouless (AT) line [14] that separates a spin-glass state in a field from a paramagnetic state. In the RSB picture for Ising spin glasses (only these will be discussed in this paper), there is a phase transition in the field h and temperature T plane separating the paramagnetic phase from a phase with RSB. In the droplet picture, the application of a field removes the phase transition to the spin-glass phase, which then occurs only in zero field, just as for the Ising ferromagnet. We have argued [15] that there is an AT line for dimensions $d > 6$ and that for $d \leqslant 6$ the droplet picture applies and the AT line is absent. The calculation involved determining the form of this line in the limit as $T \to T_c$ but what one really needs is to show that for *any* $T < T_c$, there is no transition in a field. An attempt was made to do this using a $1/m$ expansion for an m-component random field added to the m-component EA vector model [16], and once again $d = 6$ emerged as the dimension below which the droplet picture might be appropriate, but the argument is rather convoluted. A tentative argument that there might be no AT line when $d \leqslant 6$ was made by Bray and Roberts [17] when they were unable to find any stable perturbative fixed points in an ϵ expansion where $d = 6 - \epsilon$. Suggestive though these arguments, which are based on the form of the AT line or the critical exponents across it, are, they do not get really to the heart of the matter, which is the nature of the low-temperature phase in spin glasses. This is controlled by a zero-temperature fixed point, rather than a critical fixed point. In this paper we focus on this zero-temperature fixed point and its associated exponent θ.

While we believe that $d = 6$ is the dimension below which the low-temperature phase is as described by the droplet picture and above which for $d > 6$ by RSB ideas, there is clearly little chance that numerical studies could be done in such high space dimensions to confirm this changeover. However, it is possible to imagine numerical work to confirm the equivalent changeover in the one-dimensional Ising spin-glass model introduced by Kotliar *et al.* [18] given by the Hamiltonian

$$\mathcal{H} = -\sum_{i<j} J_{ij} S_i S_j, \tag{1}$$

where the Ising spins $S_i = \pm 1$ are distributed on a one-dimensional ring of length L to enforce periodic boundary conditions. The interactions J_{ij} are specified by

$$J_{ij} = c(\sigma)\frac{\epsilon_{ij}}{r_{ij}^{\sigma}}, \tag{2}$$

where [19]

$$r_{ij} = \frac{L}{\pi}\sin\left(\frac{\pi|i-j|}{L}\right) \tag{3}$$

is the chord between sites i and j. The disorder ϵ_{ij} is chosen according to a Gaussian distribution of zero mean

and standard deviation unity, while the constant $c(\sigma)$ in Eq. (2) is fixed to make the mean-field transition temperature $T_c^{\rm MF} = 1$, where $[\cdots]_{\rm av}$ represents a disorder average so that $[J_{ij}^2]_{\rm av} = c(\sigma)^2/r_{ij}^{2\sigma}$. Here $(T_c^{\rm MF})^2 = \sum_j [J_{ij}^2]_{\rm av}$. We will take $[J_{ii}^2]_{\rm av} = 0$.

The phase diagram of this model in the d-σ plane has been deduced from renormalization-group arguments in Refs. [13,19,20]. For $d = 1$, the model behaves just like the SK model when $0 \leqslant \sigma < 1/2$. For $1/2 < \sigma < 2/3$ the critical exponents at the spin-glass transition are mean-field-like, but in the interval $2/3 \leqslant \sigma < 1$, the critical exponents are changed by fluctuations away from their mean-field values. When $\sigma \geqslant 1$, $T_c(\sigma) = 0$. There is a convenient mapping between σ and an effective dimensionality $d_{\rm eff}$ of the short-range EA model [19,21–24]. For $1/2 < \sigma < 2/3$, it is

$$d_{\rm eff} = \frac{2}{2\sigma - 1}. \tag{4}$$

Thus, right at the value of $\sigma = 2/3$, $d_{\rm eff} = 6$. This mapping has a precise sense for equations associated with finite-size critical scaling at least when $1/2 < \sigma < 2/3$. Whereas for the short-range EA model there is an expression involving the dimensionality d, the corresponding formula for the Kotliar-Anderson-Stein (KAS) model is obtained by replacing d by the effective space dimension $d_{\rm eff}$ of Eq. (4) [24].

In Ref. [15] it was shown that the arguments that had led us to believe that 6 is the lower critical dimension for replica symmetry breaking, such as the form of the AT line near T_c and the Bray-Roberts study of the critical exponents across the AT line, suggested also that $\sigma = 2/3$ was the special value of σ for the KAS model. Thus, we suspect that for $\sigma < 2/3$ there is RSB in the low-temperature phase, while for $1 > \sigma \geqslant 2/3$ there is droplet behavior. The purpose of this paper is to strengthen these arguments by calculating the exponent θ of the zero-temperature fixed point. That we can do this is another advantage of the KAS model. In the droplet region, it has been realized for many years that $\theta = 1 - \sigma$ [13,20,25]. We will argue below that $\theta = 1/6$ in the RSB region, if one defines θ from the variance of the sample-to-sample free-energy differences between periodic and antiperiodic boundary conditions. For the EA model θ and d_s in the droplet regime are only known from numerical studies or simple renormalization-group approximations [26], in particular that of Migdal and Kadanoff [27].

While, in principle, the KAS model allows one to do numerical work on systems that might be the analog of high-dimensional hypercubic systems of the EA model, there are problems with its use. Finite-size effects are both large and difficult to understand and deal with. To illustrate this, we show in Fig. 1 a plot of the exponent μ (which describes the sample-to-sample variation, i.e., $\delta E \sim L^{\mu}$), δE of the ground-state energy of the system as a function of σ. The estimate of μ is obtained by just fitting δE to L^{μ}, ignoring any corrections to scaling. Clearly, the data are a long way from being satisfactorily fitted by this simple form, but if one is optimistic, one could imagine that as L is increased the results tend towards the theoretical expectation. However, the improvement is so slow we worried whether the theoretical expectation that for the SK limit $\mu = 1/6$ [28] might not be correct. In Appendix A we therefore have outlined a "rigorous"

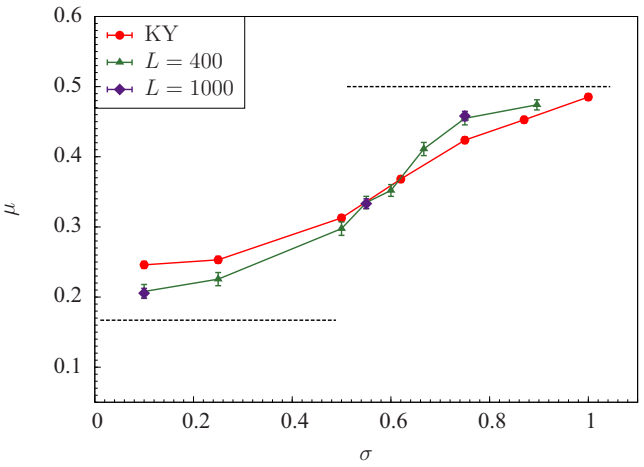

FIG. 1. Estimates of the exponent μ (sample-to-sample variation of the ground-state energy) as a function of σ, i.e., $\delta E \sim L^{\mu}$. Here KY denotes results obtained on samples up to $L = 256$ by Katzgraber and Young [19]. The expectation for μ is that $\mu = 1/6$ for $\sigma < 1/2$ [28] and $1/2$ for all $\sigma > 1/2$, as the system is now self-averaging [29] (dashed lines). Finite-size effects make the transition between these two values for μ spread over a large range of σ. Notice that the results for μ in the SK model region $\sigma = 0.1$ are moving closer to the theoretical prediction of $1/6$ as L increases.

proof that at least $\mu \leqslant 1/5$. (We put rigorous in quotes to indicate that the proof cannot be considered mathematically rigorous as it involves the use of the replica trick.) In this paper we need the value of μ as we argue that for all $\sigma < 2/3$, θ takes the SK limit value of μ.

II. INTERFACE FREE ENERGY

One of the key concepts in the droplet picture of spin glasses is the interface free energy [9–11,13,30] δF and the associated stiffness exponent θ defined by

$$\delta F \sim \ell^{\theta}, \tag{5}$$

where ℓ is the length scale of the excitation or droplet (or region of flipped spins). If $\theta > 0$, the spin-glass state is stable at finite temperature, whereas if $\theta < 0$, at $T = 0$ large-scale excitations cost little energy, so the spin-glass state is unstable at finite temperature. Thus, the dimension or value of σ at which $\theta = 0$ determines the lower critical dimension of the spin glass. In this section we calculate θ *analytically* first in the RSB region $\sigma < 2/3$ and then in the droplet region ($2/3 \leqslant \sigma < 1$) for the KAS model using the replica method and the formalism of Ref. [31].

There are many ways of defining a droplet free-energy cost, but in this section we will take it to be the interface free energy defined as the root-mean-square change in the free energy of a spin glass when the boundary conditions along one direction (the z direction) are changed from periodic to antiperiodic, i.e.,

$$\delta F = \sqrt{\overline{\Delta F_{\rm P,AP}^2}}. \tag{6}$$

Here and in the following, the overbar represents averaging over bond configurations, where $\Delta F_{\rm P,AP} = F_{\rm P} - F_{\rm AP}$, and $F_{\rm P}$ and $F_{\rm AP}$ are the free energies with periodic and antiperiodic

boundary conditions, respectively. Antiperiodic boundary conditions can be realized by reversing the sign of the bonds crossing a diameter of the ring in the KAS model. It follows that $\overline{\Delta F_{\mathrm{P,AP}}} = 0$.

The basic strategy of Ref. [31] was to replicate the system with periodic boundary conditions n times and the system with antiperiodic boundary conditions m times and keep n distinct from m. Expanding the replicated partition function in powers of m and n and taking the logarithm, we obtain

$$-\ln \overline{Z_{\mathrm{P}}^n Z_{\mathrm{AP}}^m} = (n+m)\beta\overline{F} - \frac{(n+m)^2}{2}\beta^2\overline{\Delta F^2} + \frac{nm}{2}\beta^2\overline{\Delta F_{\mathrm{P,AP}}^2} + \cdots, \tag{7}$$

where $\overline{\Delta F^2} = \overline{F_{\mathrm{P}}^2} - \overline{F_{\mathrm{P}}}^2 = \overline{F_{\mathrm{AP}}^2} - \overline{F_{\mathrm{AP}}}^2$ is the (mean-square) sample-to-sample fluctuation of the free energy, the same for both sets of boundary conditions P or AP, and $\overline{F} = \overline{F_{\mathrm{P}}} = \overline{F_{\mathrm{AP}}}$. Hence, to find the variance of the interface free energy $\overline{\Delta F_{\mathrm{P,AP}}^2}$ (which scales with L as $L^{2\theta}$), we expand $\ln \overline{Z_{\mathrm{P}}^n Z_{\mathrm{AP}}^m}$ to second order in the numbers of replicas n and m, separate out the pieces involving the *total* number of replicas $n+m$, and take the remaining piece, which is proportional to nm.

Using the standard replica field theory [32], we write

$$\overline{Z_{\mathrm{P}}^n Z_{\mathrm{AP}}^m} = \int \mathcal{D}q \exp(-\beta\mathcal{H}_{\mathrm{rep}}), \tag{8}$$

where $\mathcal{H}_{\mathrm{rep}}$ is the replica free energy, expressed in terms of the spin-glass order parameter field $q_{\alpha\beta}(x)$. For the short-range KAS model it is given by

$$\beta\mathcal{H}_{\mathrm{rep}} = \int dz \Bigg[-\frac{\tau}{2}\sum_{\alpha,\beta} q_{\alpha\beta}^2 + \frac{1}{4}\sum_{\alpha,\beta}(\partial q_{\alpha\beta}/\partial z)^2 - \frac{w}{6}\sum_{\alpha,\beta,\gamma} q_{\alpha\beta}q_{\beta\gamma}q_{\gamma\alpha} - \frac{y}{12}\sum_{\alpha,\beta} q_{\alpha\beta}^4 \Bigg], \tag{9}$$

where $q_{\alpha\beta}$ is a symmetric matrix with $q_{\alpha\alpha} = 0$, we have omitted some irrelevant terms of order q^4, and we have set $\tau = 1 - T/T_c$. The fourth-order term included is the one responsible for replica symmetry breaking in the SK model. The coefficients w and y are arbitrary positive parameters. For the short-range KAS model, the bare propagator is $g = 1/(k^2 - \tau)$.

To describe the long-range KAS model we replace the gradient terms in Eq. (9) by

$$-\frac{1}{4}\sum_{\alpha,\beta}\int_{-L/2}^{L/2} dz \int_{-L/2}^{L/2} dz' \frac{[q_{\alpha,\beta}(z) - q_{\alpha,\beta}(z')]^2}{[(L/\pi)\sin(\pi(z-z')/L)]^{2\sigma}}, \tag{10}$$

which on Fourier transforming can be seen to lead to a bare propagator of the form $g = 1/(k^{2\sigma-1} - \tau)$ [33] as $k \to 0$. [Actually Eq. (10) as it stands generates a numerical factor of $c_g(\sigma) = -\Gamma(1-2\sigma)\sin(\pi\sigma)$ in front of the $k^{2\sigma-1}$ in the propagator, which can be removed if desired by dividing Eq. (10) by $c_g(\sigma)$.] In terms of the original spins Eq. (10) is just

$$-\frac{1}{4}\sum_{\alpha,\beta}\sum_{i,j}\frac{[J_{ij}^2]_{\mathrm{av}}}{\left(T_c^{MF}\right)^2}\left(S_i^{(\alpha)}S_i^{(\beta)} - S_j^{(\alpha)}S_j^{(\beta)}\right)^2. \tag{11}$$

The replica indices go $\alpha,\beta,\gamma = 1,2,\ldots,n,n+1,\ldots,n+m$. The order parameter q divides naturally into blocks of size n and m. From now on, greek indices label the first block and roman ones the second block, so, for example, $q_{\alpha a}$ means $\alpha \in [1,n]$ and $a \in [n+1,n+m]$ and refers to the respective entry in the off-diagonal or mixed sector.

Along the z direction, which we take to be a distance along the circumference of the ring of length L, we impose the boundary condition that the solution is periodic in the greek and roman sectors and is antiperiodic in the mixed sectors reflecting the sign reversal of the bonds across the chosen diameter of the ring in the one sector with respect to the other:

$$\begin{aligned} q_{\alpha\beta}(z) &= q_{\alpha\beta}(z+L), \\ q_{ab}(z) &= q_{ab}(z+L), \\ q_{\alpha a}(z) &= -q_{\alpha a}(z+L). \end{aligned} \tag{12}$$

At mean-field level, there is the following *stable* solution for $\ln \overline{Z_{\mathrm{P}}^n Z_{\mathrm{AP}}^m}$:

$$-\ln \overline{Z_{\mathrm{P}}^n Z_{\mathrm{AP}}^m} = \beta\mathcal{H}_{\mathrm{rep}}\{q^{\mathrm{SP}}\}, \tag{13}$$

where

$$q^{\mathrm{SP}} = \left(\begin{array}{c|c} Q_{\alpha\beta}^{(n)} & 0 \\ \hline 0 & Q_{ij}^{(m)} \end{array}\right) \tag{14}$$

is independent of the spatial coordinates. It is natural that the diagonal blocks are the same as the regular Parisi ansatz because ordering in the system with periodic boundary conditions, say, should not be affected by there being another *completely independent* copy with different boundary conditions. Choosing the mixed greek-roman sector to vanish seems to be consistent with the standard interpretation [34] of RSB in short-range systems, namely, that changing the boundary conditions changes the system *everywhere*. More precisely the surface of the domain wall separating the regions that flip from the regions that do not flip is space filling. In this situation, one can reasonably expect zero overlap between configurations with different boundary conditions. However, in the droplet regime, where there is but one state and its time reversed, we still expect that the thermal average of the off-diagonal term remains zero. Our numerical work is consistent with this assumption.

At mean-field level the solution is *identical* to the customary mean-field solution but for an $(n+m)$-times replicated system ($n+m$ being finite) *without* boundary condition changes. We can therefore immediately use the result from Ref. [35] that on the mean-field level, there is no term of order $(n+m)^2$, let alone of order nm, and thus the interface energy vanishes to this order.

We now turn to the loop expansion about the saddle point, which we expect to be valid for $\sigma < 2/3$. The first correction is due to Gaussian fluctuations around the saddle-point solution. They are given by

$$-\ln \overline{Z_{\mathrm{P}}^n Z_{\mathrm{AP}}^m} = \beta\mathcal{H}_{\mathrm{rep}}\{q^{\mathrm{SP}}\} + \frac{1}{2}\sum_k I(k^{2\sigma-1}), \tag{15}$$

where

$$I(k^{2\sigma-1}) = \sum_\mu d_\mu \ln(k^{2\sigma-1} + \lambda_\mu). \tag{16}$$

Here λ_μ are the eigenvalues of the Hessian, evaluated at the saddle-point solution and d_μ are their respective degeneracies. These are the same as for a system of size $n+m$ without boundary condition changes because the saddle-point solution is the same. Only the nature of the k vectors changes for the terms involving eigenvalues whose corresponding eigenvectors f are nonzero exclusively in the mixed sector (i.e., $f_{\alpha\beta} = f_{ij} = 0$): The wave vectors have to respect the imposed boundary conditions, which implies $k = (2n_d+1)\pi/L$ (with $n_d \in \mathbb{Z}$) in the mixed sector as opposed to $k = 2n_d\pi/L$ in the greek or roman sectors.

Following Refs. [31,35], it is convenient to introduce the function

$$J(k^{2\sigma-1}) := \ln\left(k^{2\sigma-1} + \frac{x_1^2 w^2}{2y}\right) - \frac{4w(4yk^{2\sigma-1} + wx_1)}{4yk^{2\sigma-1}\sqrt{4yk^{2\sigma-1} + w^2x_1^2}} \times \tan^{-1}\frac{wx_1}{\sqrt{4yk^{2\sigma-1} + w^2x_1^2}},$$

where x_1 is the breakpoint of the Parisi q function. This is because the quadratic terms in n and m in I are of the form

$$\frac{(n+m)^2}{2} J_{\rm P}(k^{2\sigma-1}) + nm[J_{\rm AP}(k^{2\sigma-1}) - J_{\rm P}(k^{2\sigma-1})].$$

The subscripts P and AP on J mean that J must be taken as 0 when the argument is not of the required type, i.e., periodic or antiperiodic.

We can now identify the term that gives rise to the interface free energy. Comparison with Eq. (7) shows

$$\beta^2\overline{\Delta F^2_{\rm P,AP}} = \left(\sum_{\rm AP} - \sum_{\rm P}\right) J(k^{2\sigma-1}) = 2\sum_{r=1}^{\infty}\left\{J\left[\left(\frac{(2r+1)\pi}{L}\right)^{2\sigma-1}\right] - J\left[\left(\frac{(2r)\pi}{L}\right)^{2\sigma-1}\right]\right\} + \Delta f^2_{\rm SK} L^{2\mu}, \quad (17)$$

where the subscripts on the sums indicate the nature of the allowed k vectors, as made explicit in the second part of Eq. (17). The sum over k has been changed from $\pm\infty$ to 1 to ∞ with the sum multiplied by a factor of 2. The term $\Delta f^2_{\rm SK} L^{2\mu}$ in Eq. (17) comes from the $k = 0$ term in $\sum_{\rm P}$, which is nominally divergent as $k \to 0$.

In Ref. [31] we made an attempt at using finite-size ideas to regularize this divergence, but did it incorrectly. It was pointed out, correctly however, that the diverging term is identical to the variance of the sample-to-sample fluctuations of the free energy of the SK model containing L spins, $\Delta f^2_{\rm SK} L^{2\mu}$, with $\Delta F_{\rm SK}$ an L independent term. Since that paper was written, this variance has become better understood. Parisi and Rizzo [28] argued that $\mu = 1/6$. Aspelmeier [36,37] has shown that at least $\mu \leqslant 1/4$. In Appendix A the bound is strengthened; $\mu \leqslant 1/5$. We will take it that $\mu = 1/6$.

Because $J(k^{2\sigma-1}) \approx -\pi w/4yk^{2\sigma-1}$ for small k, the term in the sum in Eq. (17) is well approximated by

$$\frac{-\pi w}{4y} 2\sum_{r=1}^{\infty}\left[\frac{1}{\left[\frac{(2r+1)\pi}{L}\right]^{2\sigma-1}} - \frac{1}{\left[\frac{(2r)\pi}{L}\right]^{2\sigma-1}}\right] = CL^{2\sigma-1},$$

where $C = [1 - 4^{-\sigma}(-4+4^\sigma)\zeta(2\sigma-1)]\pi w/(2\pi^{2\sigma-1}y)$. This gives

$$\beta^2\overline{\Delta F^2_{\rm P,AP}} = \Delta f^2_{\rm SK} L^{2\mu} + CL^{2\sigma-1}. \quad (18)$$

Provided that $\mu = 1/6$, the right-hand side of Eq. (18) is dominated by the first term. It is overtaken by the second term only when $\sigma > 2/3$, but when $\sigma > 2/3$ one is in the droplet region and the calculation of the interface free energy $\beta^2\overline{\Delta F^2_{\rm P,AP}}$ takes a quite different form, as we will discuss below.

In the EA d-dimensional version of the calculation, which was summarized in Ref. [38], there was a similar change at $d = 6$ dimensions. For the EA model the system is of length L in the z direction, the direction in which the change is made from periodic to antiperiodic boundary conditions, and it is periodic and of length M in the transverse $d-1$ dimensions, so $N = LM^{d-1}$. Then, for $d > 6$,

$$\beta^2\overline{\Delta F^2_{\rm P,AP}} = \Delta f^2_{\rm SK} N^{2\mu} + L^2 f(L/M). \quad (19)$$

The term $\sim L^2 f(L/M)$ is the analog of the term $L^{2\sigma-1}$ for the KAS model and is subdominant to the term of order $N^{1/3}$ (if $\mu = 1/6$) until the dimensionality d is lowered to 6. This term depends on the shape of the system L/M and has the aspect-ratio scaling form expected for the interface free energy in dimensions $d \leqslant 6$. The leading term in $N^{1/3}$ depends only on the total number of spins N and arises because the domain walls are space filling for $d > 6$, with $d_s = d$. The interchange between the term in $N^{1/3}$ and its leading correction is one of the reasons that we suspect that 6 is the dimension below which RSB behavior changes to droplet behavior. For the KAS model, it is one of the reasons why we believe that RSB behavior does not occur in the spin-glass phase for $\sigma \geqslant 2/3$.

The key assumption used in our calculation is that in the greek-roman sector $Q_{\alpha a} = \langle q_{\alpha a}(z)\rangle = 0$. This assumption allowed us to expand about a spatially uniform solution. In Appendix B we give the numerical details of the simulations that were done to directly test this assumption. We study the three overlap functions $P^{\pi,\pi}(q)$, $P^{\pi,\overline{\pi}}(q)$, and $P^{\overline{\pi},\overline{\pi}}(q)$. Thus, the overlap q between the spin $S_i^{(\pi)}$ in the system with periodic boundary conditions and the spin $S_i^{(\overline{\pi})}$ at the same site i in the system with antiperiodic boundary conditions is defined as

$$q = \frac{1}{L}\sum_i^L S_i^{(\pi)} S_i^{(\overline{\pi})}. \quad (20)$$

The distribution of this overlap is $P^{\pi,\overline{\pi}}(q)$ and together with the similarly defined overlap distributions $P^{\pi,\pi}(q)$ and $P^{\overline{\pi},\overline{\pi}}(q)$ is shown in Figs. 2 and 3 for a variety of system sizes L and σ values. We refer to the last two distributions as the diagonal contributions [after bond averaging $P^{\pi,\pi}(q) = P^{\overline{\pi},\overline{\pi}}(q)$] and $P^{\pi,\overline{\pi}}(q)$ as the off-diagonal contribution. In replica language, the overlap defined in Eq. (20) relates to that in the mixed greek-roman sector $q_{\alpha a}$. Our crucial assumption was that

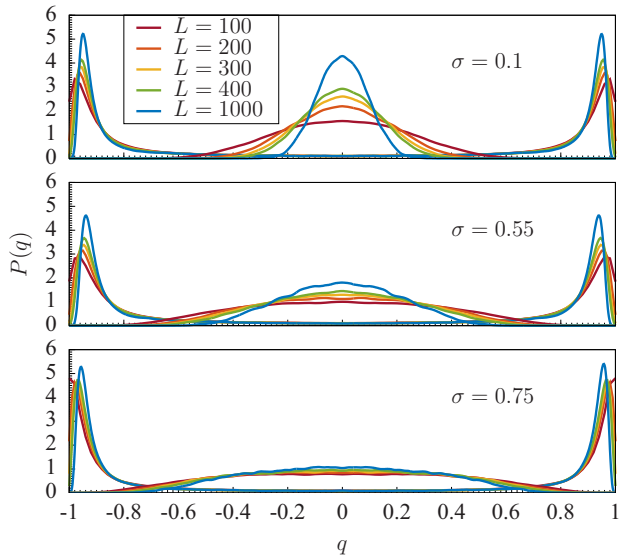

FIG. 2. Spin overlap distributions for three values of σ as a function of L at $T = 0.2T_c$. The distributions include $P^{\pi,\pi}(q)$, $P^{\overline{\pi},\overline{\pi}}(q)$, and $P^{\overline{\pi},\overline{\pi}}(q)$. The diagonal distributions have substantial peaks close to ± 1, with decreasing $q_{\rm EA}$ as L increases, while the off-diagonal distributions $P^{\pi,\overline{\pi}}(q)$ peak only at $q = 0$, becoming increasingly localized towards the center as L increases for the system sizes studied. Note that in the third panel, $P^{\pi,\overline{\pi}}(q)$ appears to saturate to a non-δ function. In all panels the systems sizes increase from bottom to top as seen from the center of the distribution for the cases where there is a central peak; otherwise, it is as seen from the peaks at large values of $|q|$.

$Q_{\alpha a}(z) = \langle q_{\alpha a}(z)\rangle = 0$. One might have expected that in the mixed sector $Q_{\alpha a}(z)$ is an odd function interpolating at one end of the system from $+q_{EA}$ to $-q_{EA}$ at the other end in order to satisfy the boundary conditions. However, if that were the situation, the off-diagonal distribution $P^{\pi,\overline{\pi}}(q)$ would

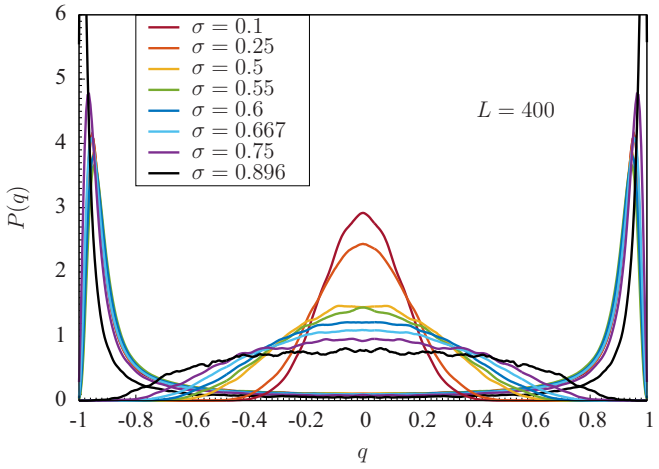

FIG. 3. Spin overlap distributions for $L = 400$ for various values of σ at $T = 0.2T_c$. The diagonal distributions are those with peaks close to ± 1, while the off-diagonal distributions $P^{\pi,\overline{\pi}}(q)$ have peaks only at $q = 0$ and become increasingly localized towards the center as σ decreases. For the distributions with a peak at the center, the values of σ increase with decreasing peak height. For the distributions with large support for $|q|$ large the values of σ increase for increasing peak height.

have peaks near $\pm q_{EA}$, just like the peaks of the diagonal distributions. However, the only peak in the off-diagonal distribution occurs at $q = 0$ and for all values of σ there are no signs of peaks at $\pm q_{EA}$. We believe that this confirms our fundamental assumption.

We find it useful to examine the second moment of $P^{\pi,\overline{\pi}}(q)$, which equals $\overline{\langle q^2\rangle}$, where

$$q^2 = \frac{1}{L^2}\sum_{j,i} S_j^{(\pi)} S_j^{(\overline{\pi})} S_i^{(\pi)} S_i^{(\overline{\pi})}. \tag{21}$$

Let us examine the situation at zero temperature. Let $\tau_i = S_i^{(\pi)} S_i^{(\overline{\pi})} = \pm 1$. Then $\tau_i = +1$ if at site i the spins associated with periodic and antiperiodic boundary conditions are parallel; $\tau_i = -1$, if these spins are antiparallel. A sequence in which the τ_i are of the same sign will be called an island. Then

$$q^2 = \left(\frac{1}{L}\sum_i \tau_i\right)^2. \tag{22}$$

For the one-dimensional KAS model with long-range interactions, a droplet may consist of disconnected pieces, i.e., islands, so a fractal dimension d_s could be defined if the number of islands scales as L^{d_s}. In the RSB region we expect that $d_s = d = 1$. If one changes the boundary conditions from periodic to antiperiodic, one does not generate a single reversed domain but instead a number of order L^{d_s} islands. The islands have a distribution of sizes. In the RSB region ($\sigma < 2/3$) we expect that the number of these islands varies as L/L_0, where $L_0(\sigma)$ is the root-mean-square size of the islands, which seems to increase with σ. This breakup into islands arises to reduce the energy by taking advantage of particular features of the bonds J_{ij} and the existence of many states in the RSB region. Because islands are only a feature of long-range one-dimensional systems, they have not been studied in the literature. In the EA model with short-range interactions, the droplets are simply connected.

The first moment of $P(q)$ equals $\overline{\langle q\rangle}$ and is zero [the functions are symmetric, so $P(q) = P(-q)$]. Thus, the average value of τ_i is zero and there are as many positive τ_i values as negative τ_i values. For any given ground state, the average of τ_i might not be zero. However, if one averages over the ground state and the states obtained by flipping all the spins in (say) the system with periodic boundary conditions, the average value of τ_i will be zero.

The second moment can be estimated by noting that the sum in Eq. (22) is a sum of L/L_0 terms random in sign and of magnitude L_0, so the sum is of order $\sqrt{L/L_0}\,L_0$. Hence, $\overline{q^2} = L_0/L$. Assuming that the distribution of q is Gaussian,

$$P^{\pi,\overline{\pi}}(q) = \sqrt{\frac{L}{2\pi L_0}}\exp\left[-\frac{Lq^2}{2L_0}\right]. \tag{23}$$

Thus, in the limit of $L \to \infty$, $P^{\pi,\overline{\pi}}(q) = \delta(q)$. The peak $P^{\pi,\overline{\pi}}(0)$ is expected to vary as $\sim\sqrt{L/L_0}$. It is shown in Fig. 4 and seems to be consistent with these arguments at least for the data for $\sigma = 0.1$ and 0.55, which lie in the RSB region.

In the droplet region the data in Figs. 2 and 3 imply that $\overline{\langle q^2\rangle}$ is nonzero as $L \to \infty$. Again, $P^{\pi,\overline{\pi}}(q)$ is a function of q centered at the origin and of nonzero width, so the peak

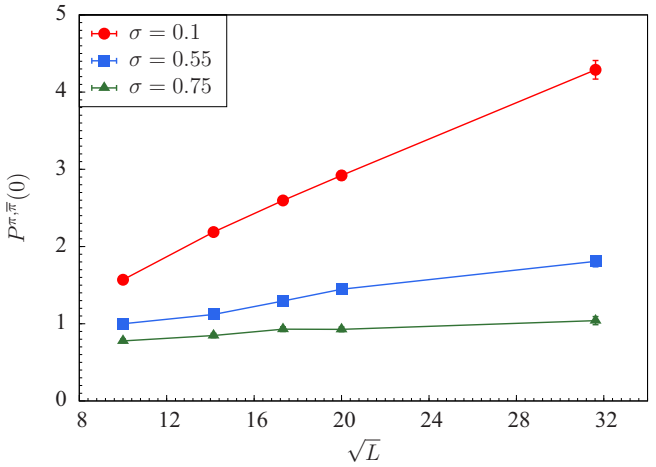

FIG. 4. Parisi overlap $P^{\pi,\overline{\pi}}(0)$ as a function of $\sqrt{L}$ for three representative values of σ at $T = 0.2T_c$. Note that $P^{\pi,\overline{\pi}}(0)$ grows approximately linearly in $\sqrt{L}$ in the RSB regime, but seems to level off in the droplet or scaling regime ($\sigma > 2/3$).

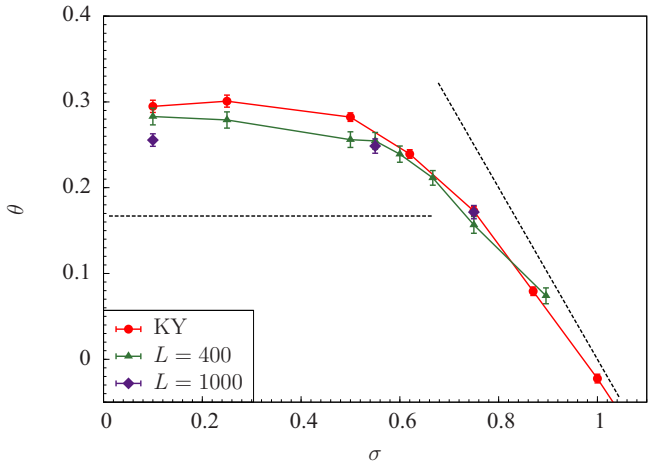

FIG. 5. Estimates of the exponent θ as a function of σ. Here KY denotes results obtained on samples up to $L = 256$ in Ref. [19] by Katzgraber and Young. The dashed line denotes the droplet regime prediction for $\theta = 1 - \sigma$. We expect this to apply for $2 > \sigma \geqslant 2/3$. When $\sigma < 2/3$ we predict that $\theta = 1/6$ and the horizontal dashed line shows this prediction. Notice that the result for θ in the SK model region ($\sigma = 0.1$) is moving closer to the theoretical prediction of $1/6$ as L increases, albeit very slowly.

$P^{\pi,\overline{\pi}}(0)$ remains finite in the droplet region. Therefore, there seems to be a simple test for determining whether the system has RSB behavior or not. If there is RSB behavior, $P^{\pi,\overline{\pi}}(0)$ diverges with the system size, whereas in the droplet region it stays finite. Simulations of the three-dimensional EA model suggest that it stays finite [39]. Our numerical work shows that in the KAS model the change from RSB to droplet behavior might occur somewhere between $\sigma = 0.55$ and $\sigma = 0.75$, but finite-size effects make it hard to pin down the change more precisely and we have failed to find any method of analysis that even hints at a sharp feature at $\sigma = 2/3$. It might be that L_0 diverges as $\sigma \to 2/3$, so that $\overline{\langle q^2 \rangle}$ joins smoothly to its expected finite form for $\sigma \geqslant 2/3$. We tried to determine whether L_0 has this feature, but failed to see it clearly, probably because of finite-size issues. We do emphasize, however, that the window $0.55 \leqslant \sigma \leqslant 0.75$ corresponds for a hypercubic system to space dimensions between approximately 4 and 10.

In the RSB region the loop expansion, i.e., the expansion about the mean-field solution, is well controlled (but technically challenging). Unfortunately, such a perturbative approach completely fails in the droplet region as the terms in the expansion about the state of assumed replica symmetry appear to break replica symmetry. This problem might be overcome by going to all orders in the expansion [40]. However, we can get the exponent θ within our formalism by using Eq. (11) for the bending energy and using the arguments in Refs. [10,13,25]. It is useful to set $\tau_i^{\alpha a} = S_i^{(\alpha)} S_i^{(a)} = \pm 1$, so that $\tau_i^{\alpha a} = +1$ if the spins $S_i^{(\alpha)}$ and $S_i^{(a)}$ are parallel and -1 otherwise. Then, by flipping (say) half the $\tau_i^{\alpha a}$ spins, one can see that the variance of the replicated bending energy scales as $mnL^{2-2\sigma}$, just as already argued in Refs. [10,13,25]. In that case

$$\theta = 1 - \sigma. \tag{24}$$

We believe that Eq. (24) applies only in the droplet region, i.e., $\sigma \geqslant 2/3$. However, in the region $\sigma < 2/3$ where we expect $\overline{\langle q^2 \rangle}$ to be of order L_0/L, the presence of so many islands (of order L/L_0) of finite size L_0 and the correlations between them must allow the system to reduce the free-energy variance associated with the transition from periodic to antiperiodic boundary conditions from this estimate of $L^{2(1-\sigma)}$ to the smaller value of $L^{1/3}$.

For $\sigma \geqslant 1$, the exponent θ is no longer positive and there will be no finite-temperature spin-glass phase [25]. However, the short-range EA model value for θ is -1 [10] and so the crossover to the short-range behavior occurs above $\sigma = 2$ when the long-range interactions become irrelevant at the zero-temperature fixed point [13,20].

III. CONCLUSION

We have predicted for the one-dimensional KAS model that in the RSB region ($\sigma < 2/3$) $\theta = 1/6$, while in the region $2/3 \leqslant \sigma < 2, \theta = (1 - \sigma)$. Notice that at the borderline of the RSB region and droplet region at $\sigma = 2/3$, θ is predicted to be discontinuous, as shown in Fig. 5.

This discontinuity seems to be a feature of the KAS model only. For the d-dimensional EA model where 6 is the borderline dimension, there is evidence that θ is continuous at six dimensions as it approaches unity in six dimensions (see Refs. [41,42] for numerical evidence on this question). If it tends to unity approaching six dimensions from below, it merges with the value of θ expected from RSB as the dimension d approaches 6 from above, as given in Eq. (19). In addition, θ and μ have been studied as a function of σ via numerical simulations. This was first done by Katzgraber and Young (KY) [19,43], with results that are not very close to the predictions made here. No discontinuity in θ was reported at $\sigma = 2/3$. We believe that the discrepancies are due to finite-size effects [24], which are surprisingly large in the KAS model. The data produced in the present study allows us to reach larger sizes than those previously studied by KY, who studied $L \leqslant 256$. The larger sizes that we studied,

$L = 400$ and $L = 1000$, do give results somewhat closer to our theoretical expectations, but the movement towards them is slow. In the droplet region the finite-size effects are probably of the same origin as those that make the Parisi overlap $P^{\pi,\pi}(q = 0)$ nonzero, contrary to the arguments of droplet theory, i.e., the system sizes studied are just not large enough to make it vanish. Smaller systems appear to have RSB features such as a nonzero value of $P^{\pi,\pi}(0)$.

In the RSB region where $\sigma < 2/3$, we predicted that $\theta = 1/6$. The value of $1/6$ is the SK value for μ. However, the values for μ mostly reported in the numerical literature [44–46] for the SK model seem closer to a value around 0.25, which, while very different from $1/6$ of the theoretical work of Parisi and Rizzo [28], is consistent with the numerical value for θ reported in [19]. However, once again, we suspect that finite-size effects in the RSB region might cause the discrepancy. In Appendix A we give what we believe is a cogent argument that at least $\mu \leqslant 1/5$.

Our work suggests that a convenient numerical test for RSB or droplet behavior is via the size dependence of $P^{\pi,\overline{\pi}}(0)$. If this quantity does not grow with system size, the ordered state is dropletlike. If it grows with system size, the system has RSB behavior. However, this test is affected by finite-size effects, yet perhaps not as badly as other commonly used tests based on the existence or not of the AT line. Simulations using special-purpose machines [47] that allow for considerably larger system sizes might allow for the detection of the true nature of the spin-glass state using the metric introduced herein.

ACKNOWLEDGMENTS

We would like to thank Stefan Boettcher for bringing us up to date on his latest numerical work and Jon Machta for a discussion regarding $P^{\pi,\overline{\pi}}(0)$ as a function of the system size L. T.A. would like to thank Christoph Norrenbrock for useful discussions. W.W. and H.G.K. acknowledge support from the National Science Foundation (Grant No. DMR-1151387). H.G.K. thanks P. Hobbs for providing multiple sources of inspiration. The work of H.G.K. and W.W was supported in part by the Office of the Director of National Intelligence (ODNI), Intelligence Advanced Research Projects Activity (IARPA), via MIT Lincoln Laboratory Air Force Contract No. FA8721-05-C-0002. The views and conclusions contained herein are those of the authors and should not be interpreted as necessarily representing the official policies or endorsements, either expressed or implied, of ODNI, IARPA, or the U.S. Government. The U.S. Government is authorized to reproduce and distribute reprints for Governmental purpose notwithstanding any copyright annotation thereon. We thank Texas A&M University for access to their Ada and Curie clusters.

APPENDIX A: "PROOF" THAT $\mu \leqslant \frac{1}{5}$ FOR THE SK MODEL

For $\sigma < 2/3$, our calculation of the exponent θ related it to the exponent μ of the sample-to-sample variation of the energy in the SK limit. This exponent is believed to be $1/6$ [28], but numerical studies of it give larger values [19,44–46]. In this Appendix we derive an upper bound on its value, namely, $\mu \leqslant 1/5$. We believe that with the methods used here it might be possible eventually to actually prove that $\mu = 1/6$. We also point out that the numerical work is done for the ground state, i.e., the the free energy at $T = 0$, and the argument in this Appendix is for the free energy at a finite temperature $T < T_c$. However, we do not think this difference affects the value of μ. The difference between the numerical value and our theoretical expectations is, we believe, just another problem caused by finite-size effects.

In Refs. [36,37] it was shown that the free-energy fluctuations ΔF in the SK model are given by the exact formula

$$\beta^2 \Delta F^2 = \frac{N^2\beta^4}{16}\int_0^\infty f_2(\epsilon)\mathbb{E}\langle(q_{13}^2 - q_{14}^2)(q_{13}^2 - q_{23}^2)\rangle\, d\epsilon + \frac{N\beta^2}{4}\int_0^\infty g_2(\epsilon)\left(\mathbb{E}\langle q_{13}^2\rangle - \frac{1}{N}\right) d\epsilon, \tag{A1}$$

where N is the system size, β is the inverse temperature, f_2 and g_2 are two functions defined by

$$f_2(\epsilon) = \frac{2\epsilon\ln(1+\epsilon^2)}{(1+\epsilon^2)^2}, \quad g_2(\epsilon) = \frac{\epsilon\ln(1+\epsilon^2)}{(1+\epsilon^2)^{3/2}},$$

and q_{ij}, with $i = 1, 2$ and $j = 3,4$, are the overlaps between spin-glass systems $1,\ldots,4$ of which systems 1 and 2 have identical Gaussian bonds $J_{kl}^{(i)}$ with unit variance, and likewise for systems 3 and 4 with bonds $J_{mn}^{(j)}$, and the correlation between the two sets of bonds is given for $k > l$ and $m > n$ by

$$\mathbb{E}\, J_{kl}^{(i)} J_{mn}^{(j)} = \delta_{km}\delta_{ln}\frac{1}{\sqrt{1+\epsilon^2}}.$$

The symbol $\mathbb{E}$ here stands for the expectation value with respect to all bonds and the angular brackets denote a thermal average. The free-energy fluctuations are thus directly linked to bond chaos via integrals over a function (f_2 or g_2) times momenta of overlaps between spin-glass replicas with different but correlated bonds.

For the calculation of Eq. (A1) it is, in principle, necessary to calculate 3- and 4-replica overlaps of the form $\mathbb{E}\langle q_{13}^2 q_{14}^2\rangle$, etc. This is, however, very difficult. Instead, we note that trivially

$$0 \leqslant (q_{14}^2 - q_{23}^2)^2 = q_{14}^4 + q_{23}^4 - 2q_{14}^2 q_{23}^2,$$

whence it follows that

$$\mathbb{E}\langle q_{14}^2 q_{23}^2\rangle \leqslant \mathbb{E}\langle q_{13}^4\rangle,$$

since replicas 1 and 2 are identical, as are replicas 3 and 4, and so $\mathbb{E}\langle q_{14}^4\rangle = \mathbb{E}\langle q_{23}^4\rangle = \mathbb{E}\langle q_{13}^4\rangle$. This implies that

$$\mathbb{E}\langle(q_{13}^2 - q_{14}^2)(q_{13}^2 - q_{23}^2)\rangle = \mathbb{E}\langle q_{13}^4 - q_{13}^2 q_{23}^2 - q_{14}^2 q_{13}^2 + q_{14}^2 q_{23}^2\rangle \leqslant 2\mathbb{E}\langle q_{13}^4\rangle. \tag{A2}$$

For an upper bound of the first integral term in Eq. (A1) it is therefore only necessary to know $\mathbb{E}\langle q_{13}^4\rangle$ as a function of ϵ. Such moments have been calculated asymptotically in various regimes in Ref. [36]. The results are summarized in Table I.

The function h is a non-negative function with the features that $h(\epsilon) = O(\epsilon^3)$ for $\epsilon \to 0$ and $h(\epsilon) \to$ const for $\epsilon \to \infty$. These results allow for calculating the asymptotic behavior of the integrals in Eq. (A1). The first integral can, with the help

TABLE I. Summary of moments $\mathbb{E}\langle q_{13}^k\rangle$ with $k = 2,4$ calculated in Ref. [36].

	Regime I	Regime II	Regime III
$\mathbb{E}\langle q_{13}^k\rangle$	$\epsilon \ll N^{-1/2}$	$N^{-1/2} \ll \epsilon \ll N^{-1/5}$	$N^{-1/5} \ll \epsilon$
$\mathbb{E}\langle q_{13}^2\rangle$	const	$\sim(N\epsilon^2)^{-2/3}$	$\sim[Nh(\epsilon)]^{-1}$
$\mathbb{E}\langle q_{13}^4\rangle$	const	$\sim(N\epsilon^2)^{-4/3}$	$\sim[Nh(\epsilon)]^{-2}$

of Eq. (A2), be bounded by

$$\begin{aligned}
&\frac{N^2\beta^4}{16}\int_0^\infty f_2(\epsilon)\mathbb{E}\langle(q_{13}^2-q_{14}^2)(q_{13}^2-q_{23}^2)\rangle d\epsilon \\
&\quad\leqslant \frac{N^2\beta^4}{8}\int_0^\infty f_2(\epsilon)\mathbb{E}\langle q_{13}^4\rangle\, d\epsilon \\
&\quad= \frac{N^2\beta^4}{8}\int_0^{N^{-1/5}} \epsilon^3\mathcal{F}(N^{1/2}\epsilon)\, d\epsilon \\
&\qquad+ \frac{N^2\beta^4}{8}\int_{N^{-1/5}}^{\epsilon_0} \epsilon^3(N\epsilon^3)^{-2}d\epsilon + O(1),
\end{aligned}$$

where $\mathcal{F}$ is a scaling function combining regimes I and II and with the properties $\mathcal{F}(x) \to$ const as $x \to 0$ and $\mathcal{F}(x) = O(x^{-8/3})$ as $x \to \infty$. The term ϵ^3 in the integrals comes from a Taylor expansion of f_2 for small ϵ. The upper limit of the second part of the integral, which corresponds to regime III, is some fixed ϵ_0 of order 1 but small enough to allow for a Taylor expansion of f_2 and h. Asymptotic evaluation of the integral is now possible and the result is, for regimes I and II,

$$\begin{aligned}
&\frac{N^2\beta^4}{8}\int_0^{N^{-1/5}} \epsilon^3\mathcal{F}(N^{1/2}\epsilon)d\epsilon \\
&\quad= \frac{\beta^4}{8}\int_0^{N^{3/10}} x^3\mathcal{F}(x)dx \sim N^{2/5}.
\end{aligned}$$

The dominant contribution to regime III of the integral comes from the lower bound and is also $\sim N^{2/5}$. A similar calculation shows that the second integral term in Eq. (A1) is subdominant to $N^{2/5}$, hence the fluctuations are bounded by

$$\beta^2\Delta F^2 \leqslant \text{const} \times N^{2/5}$$

and the fluctuation exponent μ in $\beta\Delta F \sim N^\mu$ is bounded by $\mu \leqslant 1/5$.

APPENDIX B: NUMERICAL SIMULATION DETAILS

The main purpose of the numerical work is to verify the main assumption in our calculation in Sec. II. This is that in the mixed sector $Q_{\alpha a} = \langle q_{\alpha i}(z)\rangle = 0$. It is this assumption that allowed us to construct the first term in the loop expansion about a spatially uniform solution. We also expect that $\langle q_{\alpha i}(z)\rangle = 0$ in the droplet region. Our studies of the exponents θ and μ are in effect a by-product of these investigations.

When doing numerical work on the one-dimensional long-range model, one has to decide whether to stay with the KAS model as originally outlined, in which every spin is coupled to every other spin, or the diluted model in which only a fixed number z (typically z is chosen to be 6) of the spins are coupled [21,48]. The advantage of the diluted model is that the simulations are faster, because each spin update requires only a constant number of updates from their neighbors. On the other hand, there is a consequence in that it suffers from larger finite-size effects. We therefore decided to study the fully connected model. Despite smaller system sizes than in the diluted case, finite-size corrections to scaling are smaller.

TABLE II. Parameters of the simulations for different values of σ and system size L for periodic π and antiperiodic $\overline{\pi}$ boundary conditions. Here R_0 is the population size, $T_0 = 1/\beta_0$ is the lowest temperature simulated, N_T is the number of temperatures used in the annealing schedule, and M is the number of disorder realizations.

L	σ	R_0	$1/\beta_0$	N_T	M
100	{0.1,0.25,0.5,0.55}	10^4	0.1000	101	6000
100	{0.6}	10^4	0.0934	101	6000
100	{0.667}	10^4	0.0833	101	6000
100	{0.75}	10^4	0.0690	101	6000
100	{0.896}	2×10^4	0.0373	101	12000
200	{0.1,0.25,0.5,0.55}	2×10^4	0.1000	101	6000
200	{0.6}	2×10^4	0.0934	101	6000
200	{0.667}	2×10^4	0.0833	101	6000
200	{0.75}	2×10^4	0.0690	101	6000
200	{0.896}	2×10^4	0.0373	101	6000
300	{0.1,0.25,0.5,0.55}	4×10^4	0.1000	101	6000
300	{0.6}	4×10^4	0.0934	101	6000
300	{0.667}	4×10^4	0.0833	101	6000
300	{0.75}	4×10^4	0.0690	101	6000
300	{0.896}	4×10^4	0.0373	101	6000
400	{0.1,0.25,0.5,0.55}	5×10^4	0.1000	201	6000
400	{0.6}	5×10^4	0.0934	201	6000
400	{0.667}	5×10^4	0.0833	201	6000
400	{0.75}	5×10^4	0.0690	201	6000
400	{0.896}	5×10^4	0.0373	201	6000
1000	{0.1,0.55}	2×10^5	0.1000	201	3000
1000	{0.75}	2×10^5	0.0690	201	3000

The model is simulated using the population annealing Monte Carlo method [49–52]. Population annealing works with a large population R_0 of replicas of the system, each with the same disorder. The population transverses an annealing schedule and maintains thermal equilibrium to a low target temperature $T_0 = 1/\beta_0$. In this work we used a schedule that is linear in β. When the temperature is lowered from β to β' the population is resampled. The mean number of copies of replica i is proportional to the appropriate reweighting factor $\exp[-(\beta'-\beta)E_i]$. The constant of proportionality is chosen such that the population size remains close to R_0. This is followed by $N_S = 10$ sweeps of the Metropolis Monte Carlo

TABLE III. Dependence of $T_c(\sigma)$ on σ. The values of T_c used in the simulation and the error bars are estimated using the data of Ref. [33] via a cubic spline interpolation.

σ	$T_c(\sigma)$
0.55	1.00(3)
0.6	0.93(3)
0.6667	0.83(2)
0.75	0.69(1)
0.896	0.37(1)

algorithm of each replica. We simulate M disorder realizations and measure overlaps at $T = T_0 = 0.1T_c$ and $T = 0.2T_c$. The simulation parameters are summarized in Table II. Our estimates of $T_c(\sigma)$ are given in Table III. Most of our studies of the three overlap functions were done at $0.2T_c(\sigma)$, in order to more easily compare how varying σ affects them. We find the ground-state energy by finding the lowest energy in our population at the lowest temperature and we ensure that the number of replicas having the lowest energy is large, in order to estimate the exponents θ and μ.

[1] S. F. Edwards and P. W. Anderson, Theory of spin glasses, J. Phys. F **5**, 965 (1975).

[2] G. Parisi, Infinite Number of Order Parameters for Spin-Glasses, Phys. Rev. Lett. **43**, 1754 (1979).

[3] G. Parisi, The order parameter for spin glasses: A function on the interval 0–1, J. Phys. A **13**, 1101 (1980).

[4] G. Parisi, Order Parameter for Spin-Glasses, Phys. Rev. Lett. **50**, 1946 (1983).

[5] R. Rammal, G. Toulouse, and M. A. Virasoro, Ultrametricity for physicists, Rev. Mod. Phys. **58**, 765 (1986).

[6] M. Mézard, G. Parisi, and M. A. Virasoro, *Spin Glass Theory and Beyond* (World Scientific, Singapore, 1987).

[7] G. Parisi, Some considerations of finite dimensional spin glasses, J. Phys. A **41**, 324002 (2008).

[8] D. Sherrington and S. Kirkpatrick, Solvable Model of a Spin Glass, Phys. Rev. Lett. **35**, 1792 (1975).

[9] W. L. McMillan, Domain-wall renormalization-group study of the three-dimensional random Ising model, Phys. Rev. B **30**, 476(R) (1984).

[10] A. J. Bray and M. A. Moore, in *Heidelberg Colloquium on Glassy Dynamics and Optimization*, edited by L. Van Hemmen and I. Morgenstern (Springer, New York, 1986), p. 121.

[11] D. S. Fisher and D. A. Huse, Ordered Phase of Short-Range Ising Spin-Glasses, Phys. Rev. Lett. **56**, 1601 (1986).

[12] D. S. Fisher and D. A. Huse, Absence of many states in realistic spin glasses, J. Phys. A **20**, L1005 (1987).

[13] D. S. Fisher and D. A. Huse, Equilibrium behavior of the spin-glass ordered phase, Phys. Rev. B **38**, 386 (1988).

[14] J. R. L. de Almeida and D. J. Thouless, Stability of the Sherrington-Kirkpatrick solution of a spin glass model, J. Phys. A **11**, 983 (1978).

[15] M. A. Moore and A. J. Bray, Disappearance of the de Almeida–Thouless line in six dimensions, Phys. Rev. B **83**, 224408 (2011).

[16] M. A. Moore, $1/m$ expansion in spin glasses and the de Almeida-Thouless line, Phys. Rev. E **86**, 031114 (2012).

[17] A. J. Bray and S. A. Roberts, Renormalisation-group approach to the spin glass transition in finite magnetic field, J. Phys. C **13**, 5405 (1980).

[18] G. Kotliar, P. W. Anderson, and D. L. Stein, One-dimensional spin-glass model with long-range random interactions, Phys. Rev. B **27**, 602 (1983).

[19] H. G. Katzgraber and A. P. Young, Monte Carlo studies of the one-dimensional Ising spin glass with power-law interactions, Phys. Rev. B **67**, 134410 (2003).

[20] A. J. Bray, M. A. Moore, and A. P. Young, Lower Critical Dimension of Metallic Vector Spin-Glasses, Phys. Rev. Lett. **56**, 2641 (1986).

[21] H. G. Katzgraber, D. Larson, and A. P. Young, Study of the de Almeida–Thouless Line Using Power-Law Diluted One-Dimensional Ising Spin Glasses, Phys. Rev. Lett. **102**, 177205 (2009).

[22] L. Leuzzi, G. Parisi, F. Ricci-Tersenghi, and J. J. Ruiz-Lorenzo, Ising Spin-Glass Transition in a Magnetic Field Outside the Limit of Validity of Mean-Field Theory, Phys. Rev. Lett. **103**, 267201 (2009).

[23] R. A. Baños, L. A. Fernandez, V. Martin-Mayor, and A. P. Young, Correspondence between long-range and short-range spin glasses, Phys. Rev. B **86**, 134416 (2012).

[24] T. Aspelmeier, H. G. Katzgraber, D. Larson, M. A. Moore, M. Wittmann, and J. Yeo, Finite-size critical scaling in Ising spin glasses in the mean-field regime, Phys. Rev. E **93**, 032123 (2016).

[25] M. A. Moore, Ordered phase of the one-dimensional Ising spin glass with long-range interactions, Phys. Rev. B **82**, 014417 (2010).

[26] B. W. Southern and A. P. Young, Real space rescaling study of spin glass behavior in three dimensions, J. Phys. C **10**, 2179 (1977).

[27] A. J. Bray and M. A. Moore, Lower critical dimension of Ising spin glasses: A numerical study, J. Phys. C **17**, L463 (1984).

[28] G. Parisi and T. Rizzo, Universality and deviations in disordered systems, Phys. Rev. B **81**, 094201 (2010).

[29] J. Wehr and M. Aizenman, Fluctuations of extensive functions of quenched random couplings, J. Stat. Phys. **60**, 287 (1990).

[30] J. R. Banavar and M. Cieplak, Nature of Ordering in Spin-Glasses, Phys. Rev. Lett. **48**, 832 (1982).

[31] T. Aspelmeier, M. A. Moore, and A. P. Young, Interface Energies in Ising Spin Glasses, Phys. Rev. Lett. **90**, 127202 (2003).

[32] C. de Dominicis, I. Kondor, and T. Temesvári, in *Spin Glasses and Random Fields*, edited by A. Young (World Scientific, Singapore, 1998).

[33] H. G. Katzgraber and A. P. Young, Probing the Almeida-Thouless line away from the mean-field model, Phys. Rev. B **72**, 184416 (2005).

[34] E. Marinari and G. Parisi, On the effects of changing the boundary conditions on the ground state of Ising spin glasses, Phys. Rev. B **62**, 11677 (2000).

[35] T. Aspelmeier and M. A. Moore, Free Energy Fluctuations in Ising Spin Glasses, Phys. Rev. Lett. **90**, 177201 (2003).

[36] T. Aspelmeier, Free-Energy Fluctuations and Chaos in the Sherrington-Kirkpatrick Model, Phys. Rev. Lett. **100**, 117205 (2008).

[37] T. Aspelmeier, An exact relation between free energy fluctuations and bond chaos in the Sherrington-Kirkpatrick model, J. Stat. Mech. (2008) P04018.

[38] T. Aspelmeier, A. Billoire, E. Marinari, and M. A. Moore, Finite-size corrections in the Sherrington-Kirkpatrick model, J. Phys. A: Math. Theor. **41**, 324008 (2008).

[39] W. Wang, H. G. Katzgraber, and J. Machta (unpublished).

[40] M. A. Moore, The stability of the replica-symmetric state in finite-dimensional spin glasses, J. Phys. A **38**, L783 (2005).
[41] S. Boettcher, Stiffness of the Edwards-Anderson Model in All Dimensions, Phys. Rev. Lett. **95**, 197205 (2005).
[42] S. Boettcher, Low-temperature excitations of dilute lattice spin glasses, Europhys. Lett. **67**, 453 (2004).
[43] H. G. Katzgraber and A. P. Young, Geometry of large-scale low-energy excitations in the one-dimensional Ising spin glass with power-law interactions, Phys. Rev. B **68**, 224408 (2003).
[44] S. Boettcher, Extremal optimization for Sherrington-Kirkpatrick spin glasses, E. Phys. J. B **46**, 501 (2005).
[45] H. G. Katzgraber, M. Körner, F. Liers, and A. K. Hartmann, Overcoming system-size limitations in spin glasses, Prog. Theor. Phys. Suppl. **157**, 59 (2005).
[46] S. Boettcher, Simulations of ground state fluctuations in mean-field Ising spin glasses, J. Stat. Mech. (2010) P07002.
[47] F. Belletti, M. Cotallo, A. Cruz, L. A. Fernández, A. Gordillo, A. Maiorano, F. Mantovani, E. Marinari, V. Martín-Mayor, A. Muñoz-Sudupe *et al.*, Simulating spin systems on IANUS, an FPGA-based computer, Comput. Phys. Commun. **178**, 208 (2008).
[48] L. Leuzzi, G. Parisi, F. Ricci-Tersenghi, and J. J. Ruiz-Lorenzo, Diluted One-Dimensional Spin Glasses with Power Law Decaying Interactions, Phys. Rev. Lett. **101**, 107203 (2008).
[49] K. Hukushima and Y. Iba, in *The Monte Carlo Method in the Physical Sciences: Celebrating the 50th Anniversary of the Metropolis Algorithm*, edited by J. E. Gubernatis, AIP Conf. Proc. No. 690 (AIP, New York, 2003), p. 200.
[50] E. Zhou and X. Chen, *Proceedings of the 2010 Winter Simulation Conference (WSC)* (Springer, Baltimore, 2010), p. 1211.
[51] J. Machta, Population annealing with weighted averages: A Monte Carlo method for rough free-energy landscapes, Phys. Rev. E **82**, 026704 (2010).
[52] W. Wang, J. Machta, and H. G. Katzgraber, Population annealing: Theory and application in spin glasses, Phys. Rev. E **92**, 063307 (2015).